ELSEVIER

Polymer 41 (2000) 7627–7634

polymer

# Tailored interfacial properties for immiscible polymers by hyperbranched polymers

G. Jannerfeldt, L. Boogh, J.-A.E. Månson*

*Laboratoire de Technologie des Composites et Polymères (LTC), Ecole Polytechnique Fédérale de Lausanne (EPFL), CH-1015 Lausanne, Switzerland*

Received 23 November 1999; accepted 16 February 2000

**Abstract**

The influence of hyperbranched polymer grafted polypropylene (PP–HBP) on the interfacial adhesion between fusion bonded bilayers of polypropylene (PP) and polyamide 6 (PA6) and on the properties of PP/PA6 blends was investigated. The interfacial adhesion between PP–HBP compatibilised bilayers was ten times higher compared to maleic anhydride grafted PP (PP–MAH) compatibilised bilayers. This is attributed to the higher diffusitivity and functionality of PP–HBP leading to the formation of more PP–PA6 copolymers at the interface. The elongation at break, $\epsilon_b$, of PP–HBP and PP–MAH compatibilised PP/PA6 blends were measured as a function of compatibiliser concentration. At low compatibiliser concentrations PP–HBP yielded a higher $\epsilon_b$ compared to PP–MAH, while at high concentrations similar values of $\epsilon_b$ were obtained. The higher values of $\epsilon_b$ at low concentrations are explained by the higher functionality of PP–HBP yielding more copolymers and a higher interfacial adhesion. The similar values obtained at high concentrations show that similar properties are achieved for copolymer saturation at the interface using either compatibiliser. The high diffusitivity of PP–HBP is an asset for multilayer film extrusion, while for blends, the high functionality permits the use of less compatibiliser for similar property improvements. 

*Keywords*: Interface; Blend; Compatibilisation

## 1. Introduction

There is an increasing interest in combining polymers with complementary properties. This is usually done either by blending or by multilayer film extrusion. Blending leads to a material with one phase dispersed in another, while multilayer film extrusion leads to a material with a sandwich structure. The interfacial adhesion between the phases strongly influences the final properties of the material [1]. The mechanisms through which interfacial adhesion occurs are numerous and depend on the polymers and the processing conditions. Interdiffusion of polymer chains is an efficient bonding mechanism which may occur if the polymers are brought into intimate contact above the melting temperature. The level of interdiffusion depends on the molecular weight and the miscibility of the constituents. For immiscible thermoplastic polymer pairs, however, the extent of interdiffusion is very low [2], leading to poor interfacial adhesion. On the other hand, a significant adhesion due to the crystallisation of one polymer in the presence of a second polymer in the molten state may also occur for semi-crystalline polymers [3–5]. This increased adhesion results from local volume contraction upon crystallisation increasing the interfacial area and creating mechanical interlocking. Finally, chemical and physical interactions, which can be created at the interface, can strongly contribute to the interfacial adhesion and have extensively been used to improve the adhesion between polyolefines and other engineering thermoplastics [5–8]. This is studied here in the case of polypropylene/polyamide 6 (PP/PA6) systems.

PP and PA 6 have, in many aspects, complementary properties and much research has been devoted to combining these materials [9–12]. However, practically no adhesion between these materials occurs due to the inert nature of the PP phase. A solution to this problem is to pre-graft a small quantity of the polypropylene with a monomer able to react with the amine and/or carboxylic acid end-groups of PA6. Maleic anhydride (MAH), which can readily be grafted onto PP [13,14] and is highly reactive with amine [15], is often used for this purpose. The MAH grafted PP (PP–MAH) locates at the PP/PA6 interface during processing and forms PP–PA6 copolymers through $NH_2$/MAH reactions. In the case of blends, the PP–MAH reaches the PP/PA6 interface by mixing and shearing, where copolymers are formed instantly due to the fast $NH_2$/MAH reaction

* Corresponding author.

0032-3861/00/$ - see front matter 
PII: S0032-3861(00)00133-6

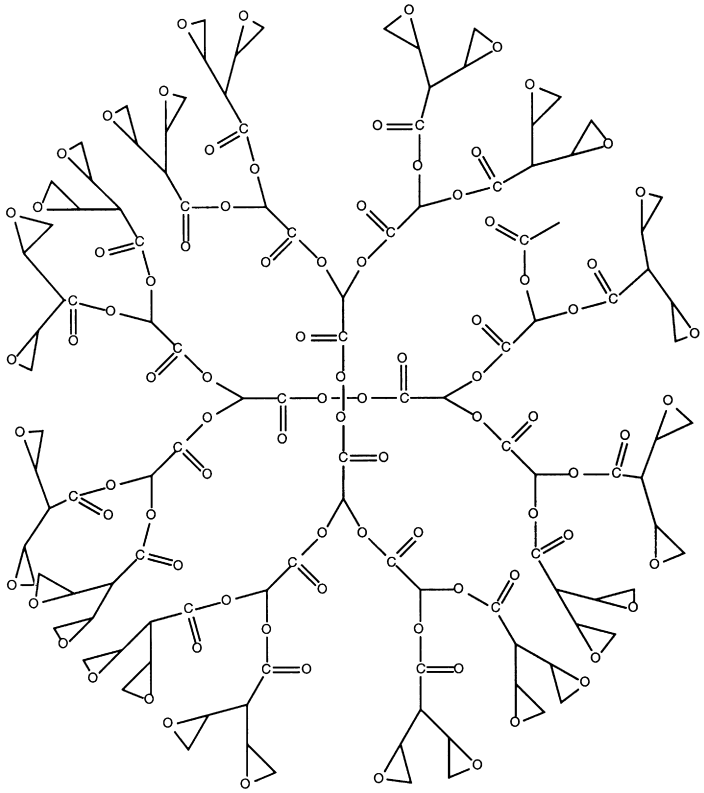

Fig. 1. Schematic of the chemical structure of the hyperbranched polymer used.

rate. The probability of a copolymer being formed increases with increasing concentration of MAH molecules grafted on the PP chain. However, the MAH grafting process onto PP involves chain cleavage [16] and the PP–MAH molecular weight is decreased with increasing MAH concentration. This decreases the efficiency of the PP–PA6 copolymers, since the entanglement ability with the PP bulk decreases with decreasing molecular weight [17]. An optimal compatibiliser would have a high molecular weight promoting efficient entanglements with the bulk and a high concentration of reactive groups to ensure that copolymers are formed within the required short processing times.

In the case of multilayer film extrusion, no dedicated mixing is present to promote transfer of the monomer grafted PP chains to the PP/PA6 interface. The copolymer formation rate is therefore governed by the thermodynamical diffusion rate of the compatibiliser through the PP phase. Since the contact time of the molten polymer layers is short for industrial multilayer co-extrusion processes, a high diffusitivity or a high concentration of the reactive monomer grafted polymers is required to obtain sufficient interfacial adhesion. The diffusion rate of PP–MAH has been shown to be low [6] and a tie-layer containing a high concentration of PP–MAH is generally used to form enough copolymers within the short processing times. The use of such tie-layers is expensive and it would be more economical to blend a compatibiliser with a higher reactivity and diffusitivity in the PP bulk during the film extrusion process.

In this paper, epoxy functional hyperbranched polymers (HBP) have been pre-grafted to PP–MAH in order to increase the compatibiliser diffusitivity and reactivity without reducing the PP chain length. The higher diffusitivity of the PP–HBP compatibiliser results from the low miscibility of the polyester based HBP in the PP phase while the higher reactivity is due to the high concentration of epoxy end-groups, which can react with both the amine and carboxylic acid end-groups of PA6 [18].

The performance of the HBP grafted PP–MAH by comparison to pure PP–MAH is investigated by characterising the interfacial adhesion between bilayers of PP and PA6 and the mechanical properties of PP/PA6 blends.

## 2. Experimental

### *2.1. Materials*

Commercial grades of PP (Appryl 3050MN1), PP–MAH (Orevac CA50) and PA6 (Orgamide RMNO) were all supplied by Elf Atochem. The HBP (Boltorn E2, Perstorp AB) used has a polyester based structure with approximately 30 epoxy end-groups as shown in Fig. 1. The HBP was pre-grafted on the PP by melt blending 9 wt% HBP and 91 wt% PP–MAH in a twin screw extruder corresponding to a HBP/MAH molar ratio of 1/3. The resulting PP–HBP molecule had a significantly higher molecular weight and

more branched structure compared to pure PP–MAH as measured by GPC. PP–HBP or PP–MAH was separately melt blended with pure PP at weight ratios of 2.5/98.5, 5/95 and 10/90 using a twin screw extruder.

### 2.2. Bilayers

Injection moulded 3 mm plaques of PP–HBP/PP (5/95), PP–MAH/PP (5/95) and pure PP were fusion bonded with 1.5 mm plaques of PA6 in an Interlaken Series 3300 load frame. Kapton tape was applied on the surfaces in contact with the mould and a 15 mm wide tape was placed between the plaques to act as a crack initiator at the interface. The plaques were placed in the pre-heated mould and a pressure of 4 MPa was applied. The mould temperature was 225°C, which is above the melting temperature of both PP and PA6. Cooling was initiated after 10 min of heating. The resulting PP/PA6, (PP–HBP/PP)/PA6 and (PP–MAH/PP)PA6 bilayers were removed after 6 min when a temperature of 40°C was reached. Two 12 mm wide bars were machined out of the bonded plates and the Kapton tape at the interface was removed. All samples were stored in a controlled atmosphere for 5 days before adhesion measurements were performed.

The interfacial fracture toughness was measured using an asymmetric double cantilever beam test by forcing a wedge along the PP/PA6 interface at a speed of 2 mm/min. The crack area in front of the wedge was measured by transmitted light, which was recorded using a video camera. The crack-area was measured at 2.5 mm intervals using image analysis software. At least 20 measurements were made for each material system with a standard deviation of ±20%. To ensure interfacial crack propagation, the thickness of the more ductile PP side was doubled compared to the PA6 side. The critical strain energy release rate, $G_{1c}$, was calculated using the following equation [19]:

$$G_{1c} = \frac{3\Delta^2 E_1 h_1^3 E_2 h_2^3}{8a^4}\left[\frac{E_1 h_1^3 C_2^2 + E_2 h_2^3 C_1^2}{(E_1 h_1^3 C_2^3 + E_2 h_2^3 C_1^3)^2}\right] \qquad (1)$$

$$C_i = 1 + \left(\frac{0.64 h_i}{a}\right)$$

where $E_i$ and $h_i$ are the Young's modulus and thickness of material $i$, respectively, $\Delta$ is the thickness of the wedge and $a$ is the average crack length. The Young's modulus for the different materials was characterised by 3-point-bending tests using a UTS load frame with a cross-head speed of 2 mm/min and a load span of 40 mm.

The interfacial morphology of the fusion-bonded plaques was investigated using a Philips EM 430 transmission electron microscope. Thin lamellas were ultra microtomed perpendicular to the interface and stained using $RuO_4$.

Electron scattering chemical analysis, ESCA, of the fractured surfaces was performed to determine the failure mode of the different samples. Photo-electron spectra for peaks of carbon, oxygen and nitrogen were recorded using a Perkin–Elmer PHI 5500 ESCA system. Prior to the measurements, the samples were stored under vacuum to avoid oxidation effects.

The number of PA6 molecules grafted at the PP/PA6 interface was estimated using ESCA. The ungrafted PA6 molecules were removed by stirring unfractured bilayer samples in formic acid for 24 h. ESCA of the uncovered PP interface were then performed, and spectra for peaks of carbon, oxygen and nitrogen were recorded. The number of PA6 molecules were determined by the relative N/C peak area following Boucher et al. [6].

### 2.3. Blends

Blends of PP/PA6, (PP–HBP/PP)/PA6 and (PP–MAH/PP)/PA6 were produced in a twin screw extruder, PRISM-16-TS. The compatibiliser concentrations used were 2.5, 5 and 10 wt% while the PA6 concentration was 20 wt% for all blends. Tensile specimens according to ASTM D638 were injection moulded and the mechanical properties of the blends were characterised by tensile tests performed on a UTS load frame at a cross-head speed of 50 mm/min.

## 3. Results and discussion

### 3.1. Bilayers

Uncompatibilised samples delaminated almost spontaneously during demoulding indicating a $G_{1c}$ value close to zero. No delamination occurred for compatibilised samples. The measured strain release values are shown in Fig. 2. The PP–HBP compatibilised sandwiches had a ten-fold higher adhesion (288 J/m$^2$) compared to PP–MAH compatibilised sandwiches (28 J/m$^2$). To explain this large difference, chemical and optical analysis of the interface was performed.

The ESCA analysis of the PP side of unfractured bilayers for which the ungrafted PA6 molecules had been removed, indicated a 4.6 times higher concentration of grafted PA6 molecules with PP–HBP compared to using PP–MAH. The higher concentration of grafted PA6 molecules with PP–HBP will contribute to altering the fracture mode and partly explains the higher adhesion values obtained.

Any eventual difference in fracture mode between the PP–HBP and the PP–MAH compatibilised samples was determined using ESCA of fractured surfaces. Photo-electron spectra of the PP side of the fusion bonded plates are shown in Fig. 3. For both PP–MAH and PP–HBP modified samples, only the carbon peak is visible meaning that the fracture propagation was either cohesive and occurred within the PP phase or was adhesive and occurred at the PP/PA6 interface. Fig. 4 shows the photo-electron spectra of the PA6 side of the fusion bonded plates and a reference spectrum of a PA6 plate before fusion bonding. The nitrogen peak, which is characteristic for PA6, is smaller but still clearly visible for the PP–MAH compatibilised fracture

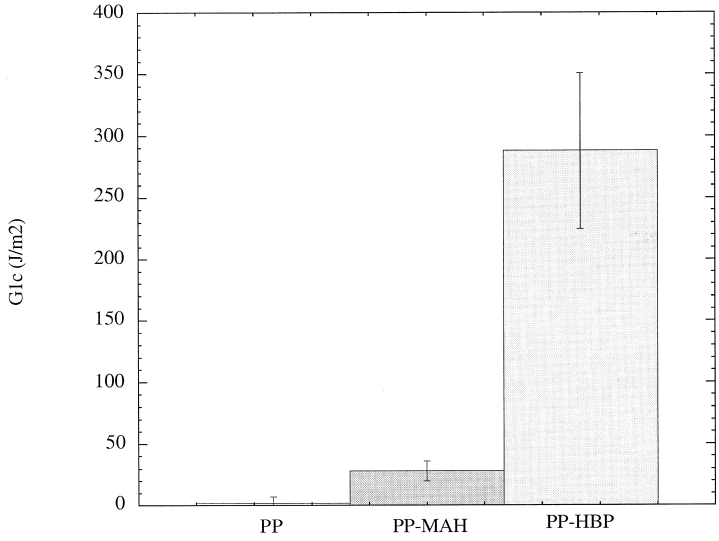


Fig. 2. Measured fracture toughness values of fusion bonded PP/PA6 bilayers.

surface. This indicates that small amounts of PP remained on the PA6 surface after failure. For the PP–HBP compatibilised fracture surface, no nitrogen peak is visible indicating the existence of a continuous and thicker layer of PP on the PA6 surface. These results show that a semi-adhesive failure has occurred in the PP–MAH compatibilised samples while a cohesive failure has occurred in the PP–HBP compatibilised samples. The thickness of the PP layer on the PP–MAH and PP–HBP compatibilised samples was determined by removing thin layers of the surface by an argon-ion sputtering gun and subsequently measuring the nitrogen content. It is assumed that no PP is present anymore when the nitrogen content remains constant. The nitrogen content as a function of depth is shown in Figs. 5 and 6, for PP–HBP and PP–MAH, respectively. A constant value of the nitrogen content was obtained at a depth of 50 nm for PP–HBP and 5 nm for PP–MAH. The gradual increase in nitrogen content for the PP–HBP modified sample indicates that an interphase layer with interpenetrated PP and PA6 phases has been formed. This was confirmed by transmission electron microscopy of the PP/PA6 interfaces of the fusion bonded samples, which are shown in Figs. 7 and 8. For both compatibilisers the phase boundary appears to be relatively sharp, indicating a low extent of interdiffusion in the solid state. However, a much more

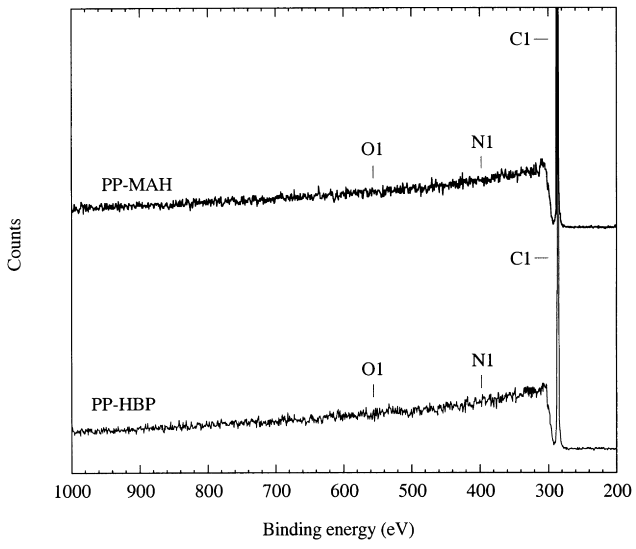


Fig. 3. Photo-electron spectra of the PP side of fractured bilayers. The upper curve represents PP–MAH modified bilayers and the lower curve represents PP–HBP modified bilayers.

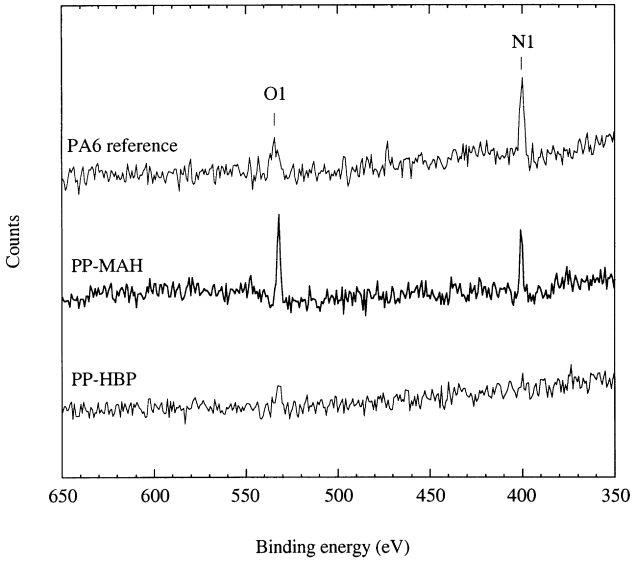


Fig. 4. Photo-electron spectra of the PA6 side of the fractured bilayers. The curve in the middle represents PP–MAH modified bilayers, the lower curve represents PP–HBP modified bilayers and the upper reference curve represents a PA6 plate before fusion bonding.

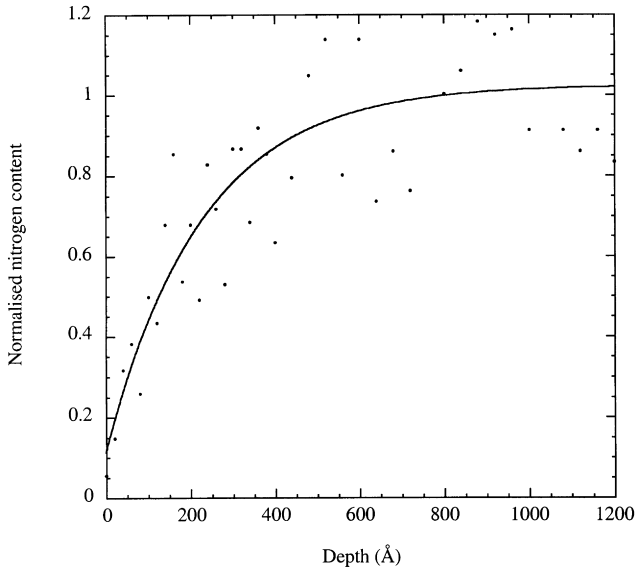


Fig. 5. The nitrogen content of the PA6 side of fractured bilayers modified with PP–HBP as a function of sputtering depth.

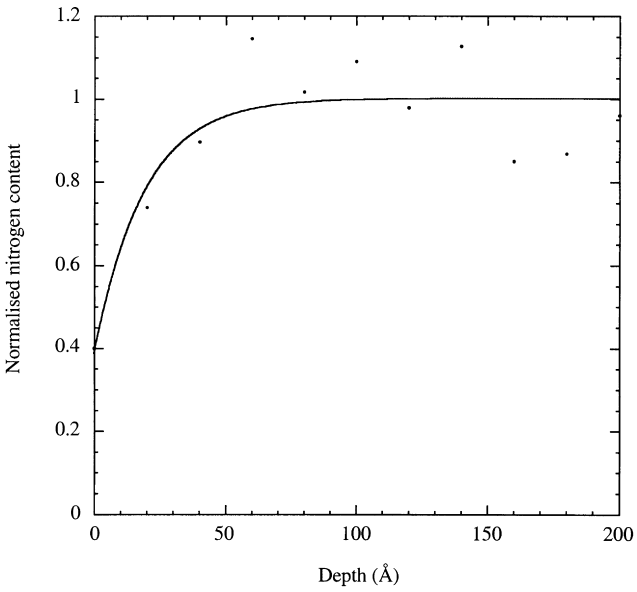


Fig. 6. The nitrogen content of the PA6 side of fractured bilayers modified with PP–MAH as a function of sputtering depth.

corrugated interface is observed for the PP–HBP modified sample. Previous work has shown that PP–HBP yields a lower interfacial tension compared to PP–MAH [18]. A lower interfacial tension has been shown to contribute to more corrugated interfaces [20,21]. The resulting larger interfacial area as well as crack deflections or even mechanical interlocking may contribute to the higher adhesion values obtained with PP–HBP.

The results presented above clearly show the efficiency of PP–HBP yielding a stronger PP/PA6 interface compared to PP–MAH. This is explained by the faster diffusion of PP–HBP leading to a higher concentration of reactive PP

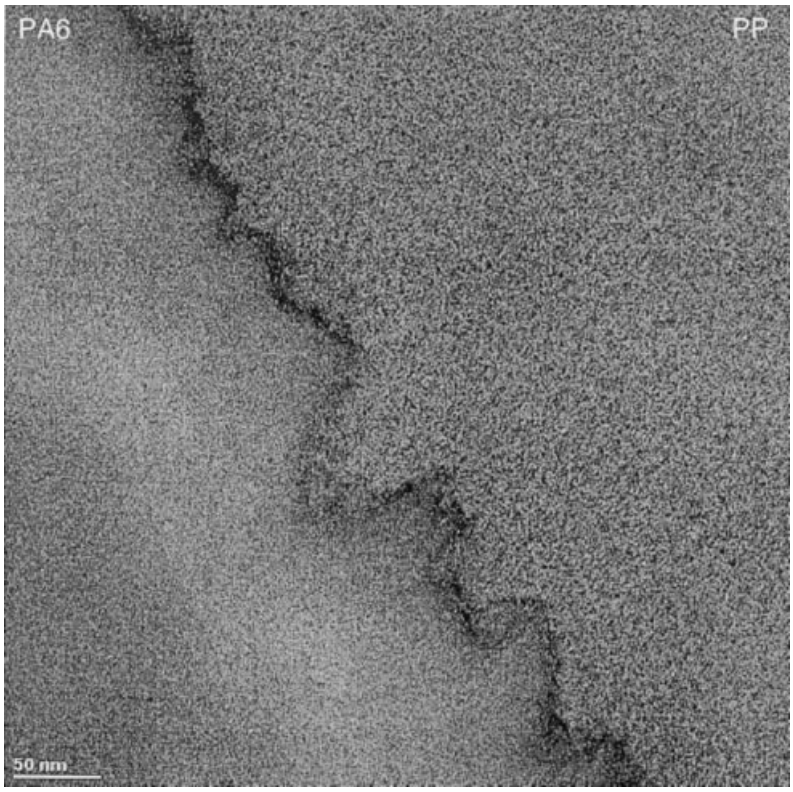


Fig. 7. Transmission electron micrograph of the interfacial region of fusion bonded bilayers compatibilised with PP–HBP.

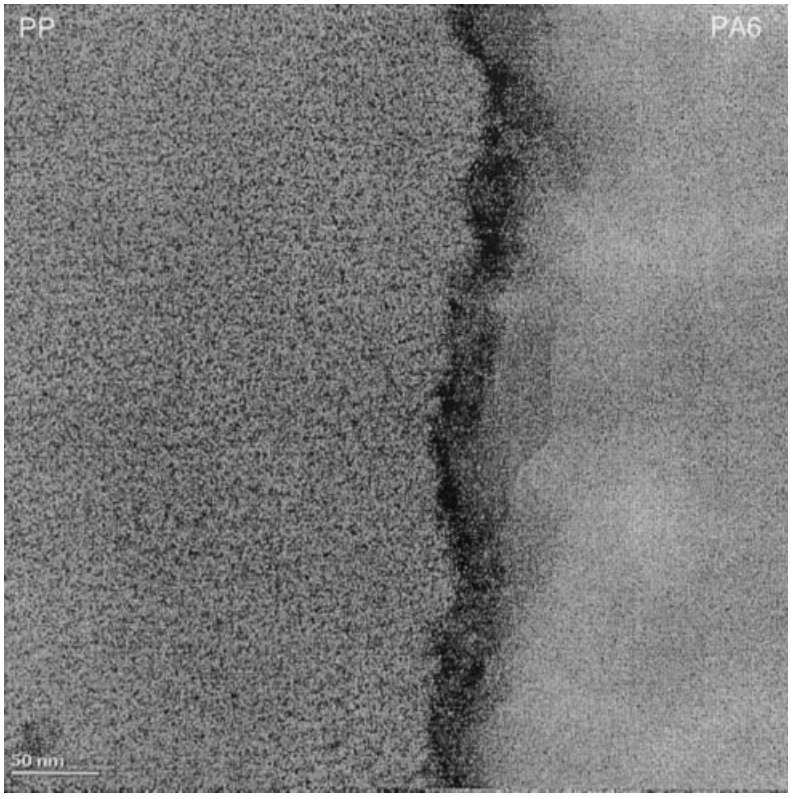


Fig. 8. Transmission electron micrograph of the interfacial region of fusion bonded bilayers compatibilised with PP–MAH.

molecules at the PP/PA6 interface and a faster copolymer formation rate [18]. The relatively low diffusion rate of PP–MAH has been illustrated previously by Boucher et al., who studied the influence of bonding time on the interfacial adhesion between PP–MAH modified PP and PA6 [7]. It was shown using similar experiments, as here, that a bonding time of 400 min was required to fully saturate the interface with compatibiliser molecules and obtain a maximal adhesion level (600 J/m$^2$). This indicates that for the bilayers tested here, which were bonded for 10 min, only a fraction of the PP–MAH molecules have diffused to the interface. Therefore, significantly higher bond strength values are expected if the interface is fully saturated with either compatibiliser molecule. The relative difference on the interfacial adhesion between PP–HBP and PP–MAH compatibilisation at interfacial saturation is discussed below.

### 3.2. Blends

During blending the compatibiliser molecules reach the phase boundaries due to mixing and shearing forces. This leads to a much faster interfacial saturation of compatibiliser than in the fusion bonding experiments presented above, where the compatibiliser reaches the interface by thermodynamical diffusion only. The increased adhesion between the phases will strongly influence the blend properties measured at high deformations. Therefore, in order to determine the relative difference between PP–HBP and PP–MAH on the interfacial adhesion at saturation, the elongation at break of PP–HBP and PP–MAH compatibilised PP/PA6 blends were measured using different compatibiliser concentrations.

The influence of the compatibiliser concentrations on the elongation at break, $\epsilon_b$, is shown in Fig. 9. For both PP–MAH and PP–HBP the $\epsilon_b$ increases with increasing concentration due to the formation of more copolymers and increasing interfacial adhesion. The $\epsilon_b$ levels off at high compatibiliser concentrations due to the appearance of interfacial saturation by the compatibiliser molecules. Interfacial saturation, however, occurs at lower concentrations for PP–HBP compared to PP–MAH. This can be explained by the more branched structure and higher molecular weight of PP–HBP, which allow fewer molecules to locate at the interface. At low compatibiliser concentrations, for which the PP/PA6 interface is not saturated with compatibiliser molecules, PP–HBP compatibilised blends had a higher $\epsilon_b$ compared to PP–MAH. Similarly, this can be attributed to the higher concentration of reactive sites of the PP–HBP allowing more PA6 molecules to react. The differences in $\epsilon_b$ between PP–HBP and PP–MAH compatibilised blends are however much smaller than the differences in $G_{1c}$ for the bilayers discussed earlier.

The higher adhesion values obtained with PP–HBP for the fusion bonded bilayers were explained by a higher diffusitivity of the PP–HBP generating more PP–PA6

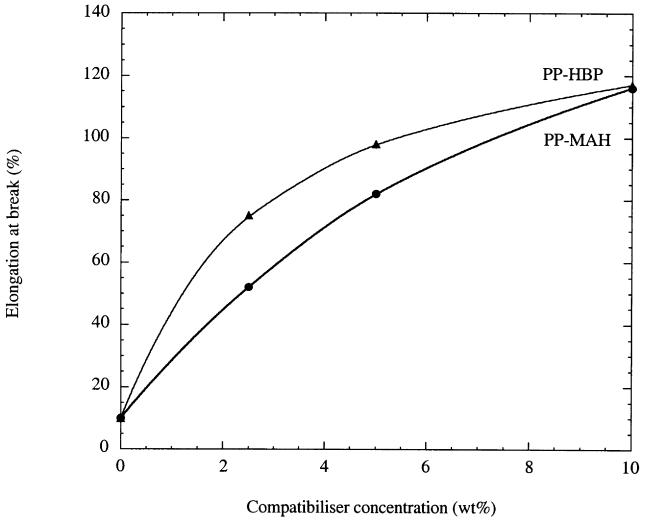


Fig. 9. Elongation at break of PP/PA6 blends as a function of compatibiliser concentration.

copolymers. For blends produced by melt mixing, the compatibiliser molecules follow the material shear flow and copolymers are formed as the compatibiliser molecules react at the interface. The copolymer formation rate during blending will therefore be much faster than during fusion bonding and depends mainly on the relative viscosities of the compatibiliser and matrix, and on the reactivity of the functional units. Cartier et al. have shown that the final morphology of PP–MAH compatibilised PP/PA6 blends is already established at an early stage in the extruder [22]. This indicates a very fast copolymer formation rate, since it can be assumed that the final morphology is established when all PP–MAH molecules have reacted or when the interface is saturated. In a comparative study, an even faster morphology development and copolymer formation rate have been shown to occur with PP–HBP due to its higher concentration of reactive groups [23]. This suggests that after extrusion both the PP–MAH and the PP–HBP have fully reacted at the interface. In the comparative study performed here, this means that the same amount of PP molecules are grafted at the interface for both PP–MAH and PP–HBP, explaining the smaller differences in $\epsilon_b$ for blends compared to $G_{1c}$ for bilayers. At high compatibiliser concentrations, for which the interface is saturated with compatibiliser molecules, similar amounts of PA6 molecules, depending on the maximum reactive group density at the interface, have reacted for both PP–HBP and PP–MAH resulting in similar $\epsilon_b$ values. It is therefore also expected that similar $G_{1c}$ values will be obtained for both PP–MAH and PP–HBP in the fusion bonding experiments, if the bonding time is increased to such an extent that both compatibilisers become saturated at the interface. In the case of PP–MAH, this was shown to occur only at times longer than 400 min [7].

For processes such as multilayer film extrusion, the contact time between the molten layers is in the order of a few seconds, interfacial saturation of the compatibiliser is thus, not likely to occur. The interfacial adhesion will therefore be governed by the ability of the compatibiliser to diffuse rapidly to the interface. For those processes, PP–HBP will have a great potential due to its high diffusitivity and high concentration of reactive groups. The results in Fig. 2 indicate that significantly shorter contact times are required for PP–HBP to achieve the same adhesion as for PP–MAH. For polymer blends, both PP–MAH and PP–HBP fully react at the interface. However, due to the higher concentration of reactive groups, lower PP–HBP concentrations are required to obtain similar mechanical properties. Fig. 9 shows that only 3 wt% is required to achieve an elongation at break of 80% with PP–HBP, while almost 5 wt% is necessary in the case of PP–MAH.

## 4. Conclusions

The interfacial adhesion between fusion bonded plaques of PP and PA6 was strongly increased with the addition of PP–HBP compared to PP–MAH. This is explained by the higher diffusitivity of PP–HBP yielding more PP–PA6 copolymers at shorter bonding times. Multilayer film extrusion processes require a high compatibiliser diffusitivity to obtain a strong interfacial adhesion within the short processing times. Due to its high diffusitivity and functionality, PP–HBP could advantageously be used for those processes allowing the use of less compatibilisers or faster processing rates.

For blends with low compatibiliser contents, PP–HBP yielded a higher elongation to break compared to PP-MAH. This is explained by a higher interfacial adhesion related to the higher concentration of reactive sites and allowing more PA6 molecules to be grafted at the interface. Thus, lower amounts of PP–HBP are required to obtain similar blend mechanical properties resulting in a cost reduction. For blends with a high concentration of compatibiliser, the interface can be expected to be fully saturated with reacted compatibiliser molecules and similar elongation to break values are obtained for both PP–MAH and PP–HBP.

## Acknowledgements

Perstorp Polyols are acknowledged for their financial support. Dr C. Plummer from the Laboratory of Polymers of EPFL is acknowledged for the TEM analysis and Mr N. Xanthopoulos from the Laboratory of Métallurgie Chimique of EPFL is acknowledged for the ESCA analysis.

## References

[1] Kryszewski M, Galeski A, Martuscelli E, editors. Polymer blends New York: Plenum Press, 1984.
[2] Jabbari E, Peppas NA. Macromol Chem Phys 1994;C34:205–41.
[3] Yuan B-L, Wool RP. Polym Engng Sci 1990;30:1454–64.

[4] Bartczak Z, Galeski A. Polymer 1986;27:544–8.
[5] Bidaux JE, Smith GD, Bernet N, Månson J-AE, Hilborn J. Polymer 1996;37:1129–36.
[6] Boucher E, Folkers JP, Hervet H, Léger L, Creton C. Macromolecules 1996;29:774–82.
[7] Boucher E, Folkers JP, Creton C, Hervet H, Léger L. Macromolecules 1997;30:2102–9.
[8] Sanches-Valdes S, Yanez-Flores I, Valle LFRD, Rodriguez-Fernandez OS, Orona-Villarreal F, Lopez-Quintanilla M. Polym Engng Sci 1998;38:127–33.
[9] Ide F, Hasegawa A. J Appl Polym Sci 1974;18:963–74.
[10] Mantia FPL. Adv Polym Tech 1993;12:47–59.
[11] Dagli SS, Xanthos M, Biesenberger JA. Polym Engng Sci 1994;34:1720–30.
[12] Hosoda S, Kojima K, Kanda Y, Aoyagi M. Polym Network Blends 1991;1:51–9.
[13] Sathe SN, Rao GSS, Devi S. J Appl Polym Sci 1994;53:239–45.
[14] Roover BD, Sclavons M, Carlier V, Devaux J, Legras R, Momtaz A. J Polym Sci: Polym Chem 1995;33:829–42.
[15] Orr CA, Adedeji A, Hirao A, Bates FS, Macosko CW. Macromolecules 1995;30:1243–6.
[16] Ho RM, Su AC, Wu CH, Chen SI. Polymer 1993;34:3264–9.
[17] Duvall J, Sellitti C, Myers C, Hiltner A, Bauer E. J Appl Polym Sci 1994;52:207–16.
[18] Jannerfeldt G, Boogh L, Månson J-AE. J Polym Sci: Polym Phys 1999;37:2069.
[19] Kanninen MF. Int J Fract 1973;9:83.
[20] Jiao J, Kramer EJ, Vos S, Möller M, Koning C. Polymer 1999;40:3585–8.
[21] Lyu S-P, Cernohous JJ, Bates FS, Macosko CW. Macromolecules 1999;32:106–10.
[22] Cartier H, Hu G-H. Polym Engng Sci 1999;39:996–1013.
[23] Jannerfeldt G, Boogh L, Månson J-AE. Polym Engng Sci. Submitted for publication.